

Explainable Artificial Intelligence for Pharmacovigilance: What Features Are Important When Predicting Adverse Outcomes?

ISAAC RONALD WARD, School of Population & Global Health, and Department of Computer Science & Software Engineering, University of Western Australia, Australia

LING WANG, School of Population & Global Health, University of Western Australia, Australia

JUAN LU, School of Population & Global Health, University of Western Australia, Australia

MOHAMMED BENNAMOUN, Department of Computer Science & Software Engineering, University of Western Australia, Australia

GIRISH DWIVEDI, Cardiology Department Fiona Stanley Hospital, Harry Perkins Institute of Medical Research, Medical School University of Western Australia, Australia

FRANK M SANFILIPPO*, School of Population & Global Health, University of Western Australia, Australia

Background and Objective

Explainable Artificial Intelligence (XAI) has been identified as a viable method for determining the importance of features when making predictions using Machine Learning (ML) models. In this study, we created models that take an individual's health information (e.g. their drug history and comorbidities) as inputs, and predict the probability that the individual will have an Acute Coronary Syndrome (ACS) adverse outcome.

Methods

Using XAI, we quantified the contribution that specific drugs had on these ACS predictions, thus creating an XAI-based technique for pharmacovigilance monitoring, using ACS as an example of the adverse outcome to detect. Individuals aged over 65 who were supplied Musculo-skeletal system (anatomical therapeutic chemical (ATC) class M) or Cardiovascular system (ATC class C) drugs between 1993 and 2009 were identified, and their drug histories, comorbidities, and other key features were extracted from linked Western Australian datasets. Multiple ML models were trained to predict if these individuals would have an ACS related adverse outcome (i.e., death or hospitalisation with a discharge diagnosis of ACS), and a variety of ML and XAI techniques were used to calculate which features — specifically which drugs — led to these predictions.

Results

The drug dispensing features for rofecoxib and celecoxib were found to have a greater than zero contribution to ACS related adverse outcome predictions (on average), and it was found that ACS related adverse outcomes can be predicted with 72% accuracy. Furthermore, the XAI libraries LIME and SHAP were found to successfully identify both important and unimportant features, with SHAP slightly outperforming LIME.

Conclusions

ML models trained on linked administrative health datasets in tandem with XAI algorithms can successfully quantify feature importance, and with further development, could potentially be used as pharmacovigilance monitoring techniques.

1 INTRODUCTION

Artificial Intelligence (AI) and Machine Learning (ML) have recently demonstrated their utility in digital health applications regarding the prediction of outcome events [1, 2]. These techniques use models

that learn patterns based on large quantities of data. These models typically demonstrate high predictive power, but they have been criticised as being 'black box' algorithms: their internal operations incomprehensible to human operators [3]. In critical decision making domains — such as healthcare — the reason for a decision is often as equally important as the decision itself.

In response, Explainable Artificial Intelligence (XAI) has experienced a surge in interest and development. XAI is a field concerned with increasing the explainability and transparency of AI algorithms, by making their influencing variables, complex internal operations, and learned decision making paths interpretable [3, 4]. Although popular XAI methods such as 'Local Interpretable Model-Agnostic Explanations' (LIME) [5] and 'SHapely Additive exPlanations' (SHAP) [6] have proven to be useful in interpreting black box models [7, 8], more needs to be understood about these methods before they can be adopted in critical decision making domains [9].

In this work, we used pharmacovigilance monitoring as the critical decision making domain which demands transparency and trust. Pharmacovigilance systems aim to recognise pharmaceutical safety issues, and thus impact human well-being, public health, pharmaceutical companies [1], policy, and regulations at the highest scale. In one case in 2004, the non-steroidal anti-inflammatory drug (NSAID) rofecoxib was withdrawn from global markets based on evidence that it could double the risk of myocardial infarction and stroke if taken for 18 months or more [10]. At this time, celecoxib, another COX-2 selective inhibitor had its sales reduced by 50% [11]. Methods which could have quantified and exposed these risks earlier would have significantly improved public health and safety, and both statistical and AI-based methods have been suggested as candidate solutions [12–18].

The objective of this study was thus two-fold. Firstly, we used ML to predict the probability of an individual having an Acute Coronary Syndrome (ACS) based adverse outcome. We did this using only administrative health data (Section 2.3). Secondly, we analysed these ML models with XAI, and confirmed that expected patterns were identified correctly (Section 2.4). Among other patterns, we expected to find that taking rofecoxib and celecoxib would lead to

*The corresponding author.

a disproportionate increase in the predicted probability of an ACS related adverse outcome.

2 METHODS

2.1 Datasets

The study dataset was prepared by linking data from local core linked administrative datasets (Western Australian Department of Health) and pharmacy dispensing data from the Australian government. All data are de-identified so as to protect sensitive information. The exposure information is provided by the Pharmaceutical Benefits Scheme (PBS) data, which contains drug dispensing data from PBS-registered pharmacies (community and hospitals). Among other variables, rows in this dataset describe drug dispensing events by their date of supply, quantity, and ATC classification system codes. The outcome events from core datasets of the Western Australian Data Linkage System (WADLS): the Hospital Morbidity Data Collection (HMDC), Emergency Department Data Collection (EDDC), and Deaths Register [19]. These datasets contain records of all admissions to public and private hospitals in Western Australia (HMDC), emergency department presentations (EDDC) and deaths, and allow us to identify events by their codes from the International Classification of Diseases 9th revision clinical modification (ICD-9-CM) and 10th revision Australian Modification (ICD-10-AM).

2.2 Data preparation

To produce data features which can be used for ML, the PBS, HMDC, EDDC, and Deaths Register data were first cleaned, with null entries being dropped entirely. Sex and age are taken from the PBS data, and entries are linked across datasets by the patient’s anonymous encrypted identification code. ATC M (musculo-skeletal system) and C (cardiovascular system) class drugs were investigated for this study, as they capture the drugs of interest (rofecoxib and celecoxib) as drugs used by patients with cardiovascular diseases. We disregard uncommon drugs with less than 10,000 total dispensing events.

ACS related hospitalisations and deaths were identified for each individual from the HMDC, EDDC, and Death Register. The study cohort included individuals who were classified as concessional beneficiaries, as their dispensing records within the PBS are more complete than individuals in the general category [20]. We additionally limit the study cohort to individuals aged over 65, as not all concessional beneficiaries are over 65. Finally, we used data from January 1st 1993 to December 31st 2009, which includes the exposure period of interest (2003-2004) with 10-year lookback for comorbidities and followup period to identify outcomes. Critically, it provides us with a large dataset suitable for ML.

The timeline in Figure 1 was used to generate the feature vectors – the first supply date of a drug is identified via the PBS data, and features are selected around this date. An individual’s comorbidity history is defined by the 10 years prior to the initial supply date, and their drug history is defined by the supply of drugs in the 6 months prior to the initial supply date. The drug exposure window is defined by the 30 days following the initial supply date, and the follow up period is the remaining 335 days in the year after the end of the drug exposure window.

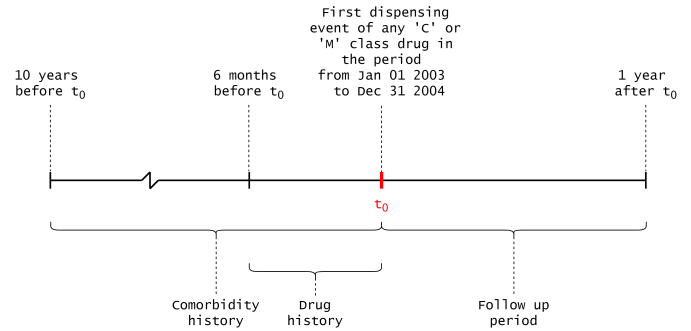


Fig. 1. The process by which dispensings, hospitalisation, and death events are converted into drug history and comorbidity history events.

Hospital admissions or emergency department presentations were considered comorbidities if they were within the 10 year comorbidity history period, and ACS related hospital admissions or deaths were considered adverse outcomes if they were within the follow up period. These conditions were identified by ICD-9-CM and ICD-10-AM codes. Similarly, any PBS dispensing events for C or M class drugs were added to an individual’s drug history if they were within the drug history period. A full list of the conditions considered as adverse outcomes, and the ATC codes of considered drugs are shown in Appendix A.

The 158-dimension, per patient, per supply feature vectors were constructed by concatenating an individual’s sex, age, drug history, comorbidities, and two additional random features. Drug history is represented by 59 counts of specific C class drug dispensings, and 19 counts of specific M class drug dispensings, where each element corresponds to a valid ATC drug code which was recorded in the PBS data. The value of each element corresponds to the number of dispensing events the individual had registered for that particular drug in the drug history period. Similarly, hospitalisation comorbidities were represented by 76 values, where each value corresponds to the number of hospitalisation events that the individual had for that specific condition in the comorbidity period. The random features were added because by definition they have no predictive power. This aids in quantifying the models’ tendency to overfit, and in quantifying the feature importance methods’ ability to detect truly important features. A random integer (in the range 0–158) and floating point number (in the range 0–1) are appended to each feature vector. Note that every feature in the feature vector is represented numerically, and that scikit-learn interprets all features as continuous numeric variables with threshold-based decision boundaries – thus preventing the possibility of bias due to data type.

The label for a feature vector was a 0 or 1 (one-hot encoding), denoting if an individual suffered an ACS related adverse outcome or death during the follow up period (1) or not (0). We removed all instances which had identical feature vectors but different labels, as these cases lacked the input information required to discriminate between the two possible outcomes. This limitation is inherent in administrative datasets; such datasets do not capture all the information about an individual that describes their full clinical history and presentation.

The resulting linked dataset is imbalanced: the number of instances which did not have ACS related adverse outcomes (the negative class) outnumbered those who did (the positive class) by a ratio 6.94:1. For the training set, we used 70% of the instances and randomly undersampled from the negative class population until the training dataset was exactly equal, totalling 278,608 instances [21]. Random undersampling approaches have been proven to be suitable for dealing with minority classes with relative class sizes that were even smaller than ours (our relative minority class size is 14.41%, and 0.1% minority classes have been trained with undersampling with minimal performance losses in [22]). Having a balanced training set will prevent the ML models from learning to predict the larger class in lieu of identifying meaningful patterns. We used 4-fold cross validation when training and testing, with a ratio of 30% of the total instances reserved for the testing set. Performance measures were averaged across folds.

2.3 Machine Learning

We used Decision Tree (DT) based classification models: **R**andom **F**orests (RFs), **E**xtra random **T**rees (ETs), and **e**Xtreme **G**radient **B**oosting machines (XGB) [23–25]. These tree based models benefit from being both widely accepted and used, as well as having accelerated feature importance value computations [6] (see Section 2.4). Moreover, using a variety of proven ML models allows us to investigate if our results are not model dependent.

A **DT** is a representation of an algorithm that follows a tree-like structure (see Figure 2). In ML, DTs can be generated from labelled datasets — during each training step, a condition is based on some selected feature (either randomly or based on some measure of optimality), and the data is split into subsets based on the outcome of this condition. Each splitting point creates new nodes, and this process continues recursively until some stopping criteria has been met (e.g. accuracy, node limits). One measure of optimality is *Gini impurity*, which measures the probability of an instance being classified incorrectly when classifying it based on the class distribution of the dataset.

It is also possible to identify the most important features by inspecting the DTs directly; the features that are used as splitting criteria in shallow nodes discriminate between feature vectors more effectively (i.e., these features have the highest *information gain*). In practice, we find that single DTs are prone to overfitting due to the small samples that occur near the tree’s leaf nodes. As such, all of our feature importance analyses are based on ensembles of trees, rather than single trees, which will ensure that the calculated feature importance scores are less variant and more indicative of the global patterns in the data.

An **RF** is an ensemble architecture which bags multiple DTs to produce more stable predictions. DTs with high complexity often overfit, whereas RFs create subsets of random features and build a greater number of smaller DTs using these subsets. This has a tendency to increase variance and thus reduce overfitting [23]. Furthermore, **ETs** further increase the variance by also randomly choosing the decision threshold at each node in each DT [24]. **XGBs** are another bagging approach to DTs, but in this case boosting is used to alter the evaluation criteria for each DT. These errors are

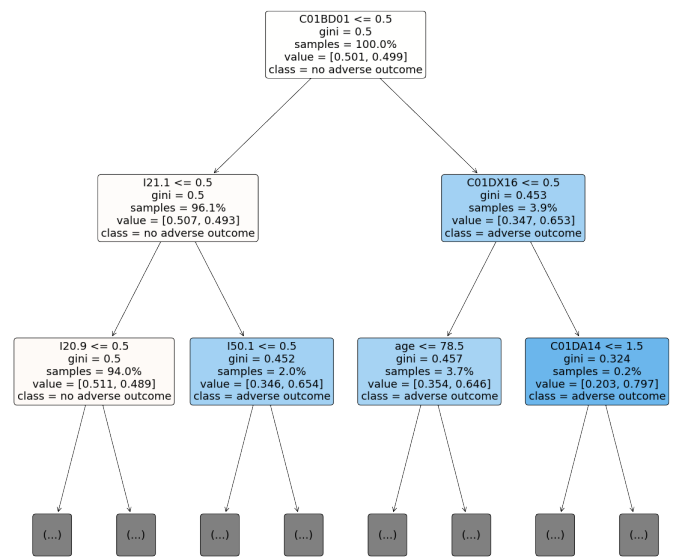


Fig. 2. Visualisation of a portion of a single DT from the trained RF used in this study. At each node, a feature and threshold is selected, for example: in the top-most node, the decision is based on whether or not an individual was dispensed C01BD01 (dofetilide) in their drug history. Other drug dispensing features, comorbidities, and the individual’s age are also used as decision features in this image. The Gini impurity, the ratio of samples which make it to that node (samples), the ratio of samples which are split into each branch of that node (value), and the majority class (class) rendered. The DT is cut off after the third ply in this figure, as the actual DT’s depth is over 30 in this case. DT, Decision Tree; RF, Random Forest.

minimised via gradient descent. XGBs have numerous performance optimisations which suit them for the purpose of this study [25, 26].

To optimally train these models we performed 128 rounds of Bayesian hyperparameter optimisation over a distribution of valid parameters (see Appendix B for the descriptions of these searches) [27]. In each round, a configuration of parameters is selected and the resulting model is trained and tested using 4-fold cross validation [28]. Performance measures were averaged across folds. The most performant model from the 128 trials is selected and its feature importance is analysed using both traditional methods and XAI (the results of which are averaged across the three models and presented in Figure 3).

2.4 Feature importance

We used ML-based feature importance methods to understand the contribution of certain features to the model’s prediction. From a pharmacovigilance perspective, we want to know which drug(s) have the highest association with the outcome. The traditional methods that we employed were measures of **M**ean **D**ecrease of **I**mpurity (MDI), and **M**ean **D**ecrease in **A**ccuracy (MDA), and the XAI-based methods are LIME and SHAP.

MDI is based on the depth of certain nodes in a tree-based model’s DTs. If a node near the top of the DT uses some criterion based on a given feature, then that feature must contribute to the final decision for a larger fraction of samples than a feature which is used lower in the DT. This fraction can be used as an estimate of a feature’s relative importance. MDI is calculated by combining the decrease in Gini impurity with this relative importance [29]. We used scikit-learn’s implementation of MDI in this study.

MDA is defined as the decrease in model accuracy on the test set when a given feature is randomised or permuted [23, 30]. The drop in accuracy indicates how much the model depends on the given feature, and thus is an estimate of feature importance. MDA benefits from being model agnostic, unlike MDI measures which need to be performed on tree-based models. Additionally, MDA does not suffer from a bias towards high cardinality features (as MDI does). The method does still suffer from some bias however – when two or more features are highly correlated, permuting one feature does not restrict the model’s access to it, as it can still be accessed via the correlated feature(s).

Local Interpretable Model-agnostic Explanations (LIME) [5] generate local surrogate models to explain individual predictions produced from ML architectures. LIME takes a single instance, and locally *perturbs* the feature values to other valid values based on the dataset. These perturbed values are then fed back into the trained model. This creates a new dataset of input to output mappings, which an interpretable model is trained on. During the training of this local surrogate model, instances are weighted by the distance of the perturbed feature to the single feature of interest. The result is a ML model which is explainable and has a high local fidelity: it approximates the black box model locally in feature space, but not globally. LIME has been noted to increase model interpretability on tabular data [9], but relies on the correct definition of the local neighborhood and is thus highly dependent on kernel parameters [31].

SHapley Additive exPlanations (SHAP) [6] assigns each input feature an importance value for a given prediction, based on principles from cooperative game theory. For any given feature vector, SHAP takes a single feature’s value and replaces it with a sampled value from the dataset. The model of interest makes a prediction for this augmented feature vector and the difference in output values – the marginal contribution – is noted. This sampling process can be repeated to improve our estimates of marginal contribution. This is repeated for all possible coalitions, and the resulting average marginal contributions to each coalition are the Shapley values. SHAP can approximate these values accurately and quickly for tree-based models.

3 RESULTS

3.1 Predicting per-patient adverse outcomes

Table 1 presents the results from the hypertuning experiments for each of the model classes. The hypertuning procedure converges each model to similar levels of accuracy and Area Under the Receiver Operating Characteristic (AUC). The XGB classifier outperforms the RF classifier, which outperforms the ET classifier.

Table 1. The test results after training the RF, ET and XGB models used in this study. For each model, a Bayesian hyperparameter optimisation search with 128 iterations was performed. Macro-average precision was used here, as this measure is **insensitive** to the imbalance of classes in the test dataset.

Model	AUC	Accuracy (%)	Macro-avg. Precision (%)	Macro-avg. Recall (%)
RF	0.70	71	67	70
ET	0.69	70	66	69
XGB	0.72	72	68	72

AUC, Area under the ROC Curve; RF, Random Forest; ET, Extra Trees (classifier); XGB, Extreme Gradient Boosting.

3.2 Generating feature importance for pharmacovigilance

We analysed the models’ feature importance scores using the four measures described in Section 2.4. The per-feature importance scores as determined by MDI, MDA, LIME, and SHAP are plotted in Figure 3. There is an important distinction here: for MDI and MDA measures, we showed the importance of any feature when making either an adverse outcome *or a non adverse outcome prediction*, as these measures do not give per-instance feature contributions. For LIME and SHAP, we present results for specifically making adverse outcome predictions, and we note that it is possible for a feature to attain on-average negative contribution to an ACS related adverse outcome prediction (these features ‘protect’ a patient from having an ACS related prediction).

We observed that age and sex are almost always attributed with a high importance – in MDI and MDA especially, but less so under LIME analysis. There are repeating peaks and patterns of importance across MDI, MDA, LIME, and SHAP in C class drug history, M class drug history, and ICD-10-AM codes (see Figure 3 and Appendix A for more detail). Rofecoxib and celecoxib are the most important M class drug history features under MDI and MDA analysis, but not so under LIME analysis. Under SHAP analysis, rofecoxib and celecoxib are the second and third M class drug history features that on average contribute to an adverse outcome prediction respectively, being slightly behind M05BA04 (alendronic acid), with the feature importance scores of rofecoxib and alendronic acid being 1.16×10^{-4} and 1.19×10^{-4} respectively. We note the random features’ importances under MDI analysis, which is a result of the method’s bias towards high cardinality features [30].

We further analysed the feature importance rankings at the model level by displaying the key feature importance rankings in Table 2. The results largely reflect the average results, but the XGB classifier notably disfavors random features under MDI analysis, and favors the random floating point feature under MDA and SHAP analysis. We note that different model types may correlate to the features that are considered important – even across feature importance methods. This is potentially due to inductive bias in the learning algorithm’s design. Indeed, RFs and ETs are algorithmically similar, with the only key difference being the randomisation of selected thresholds and the sampling methods used in ETs.

We also provide the per-model rankings of the M class drug features in Table 3, and we observe that the XGB model disagrees with the RF and ET models under MDI analysis, but agrees with the RF and ET models under MDA analysis. This is potentially due to the shortcomings of MDI compared to MDA, which are discussed in the next section. LIME analysis suffers from high variance and inconsistency in the results, potentially due to the method’s high local fidelity. SHAP analysis results are largely consistent, apart from the RF not identifying celecoxib dispensing as an important feature whereas the ET and XGB models both do.

Table 2. Rankings of features as measured by MDI, MDA, LIME, and SHAP. Key confounders sex and age are expected to be ranked highly, and random features to be ranked lower.

Measure	Feature	Overall ranking (out of 158)			
		RF	ET	XGB	Avg.
MDI	sex	8	4	5	5
	age	1	1	20	1
	random float	3	20	113	8
	random int	4	21	116	10
MDA	sex	4	2	5	2
	age	1	1	1	1
	random float	157	158	43	157
	random int	158	157	158	158
LIME	sex	29	37	46	40
	age	43	53	63	57
	random float	42	56	72	61
	random int	75	101	84	86
SHAP	sex	7	2	7	5
	age	1	1	13	10
	random float	155	128	20	35
	random int	150	114	126	139

The average score is not the average rank, but the rank of the average importance for all models across that measure, as rendered in Figure 3. The feature with the highest importance is ranked as 1, and the lowest as 158. MDA, Mean Decrease in Impurity; MDA, Mean Decrease in Accuracy; LIME, Local Model Agnostic Explanations; SHAP, Shapley Additive Explanations; RF, Random Forest; ET, Extra Trees (classifier); XGB, Extreme Gradient Boosting

3.3 Stratified analysis using Explainable Artificial Intelligence

The XAI methods LIME and SHAP can extract per-instance prediction contributions, which allowed us to focus our analysis on the *values* of certain features (i.e., we can investigate local, rather than global importance scores). We divided the test datasets into four distinct strata, depending on whether or not an individual was or was not dispensed celecoxib or rofecoxib. For this analysis, we focussed on the M class drugs and present these findings in Figure 4. We observed that rofecoxib and celecoxib dispensings increases the likelihood of an adverse outcome prediction, and that *not* having

Table 3. The rankings of the M class drug history features specifically, as measured by MDI, MDA, LIME, and SHAP. The feature with the highest importance is ranked a 1, and the lowest as 19. The drugs of interest to this study — celecoxib and rofecoxib — have their importances across all models shown. The average score is not the average rank, but the rank of the average importance for all models across that measure, as rendered in Figure 4.

Measure	Feature	M class drug ranking (out of 19)			
		RF	ET	XGB	Avg.
MDI	celecoxib	1	2	18	1
	rofecoxib	2	1	17	2
MDA	celecoxib	1	2	1	1
	rofecoxib	2	3	3	2
LIME	celecoxib	15	9	10	12
	rofecoxib	4	11	12	9
SHAP	celecoxib	10	4	3	3
	rofecoxib	1	2	1	2

MDA, Mean Decrease in Impurity; MDA, Mean Decrease in Accuracy; LIME, Local Model Agnostic Explanations; SHAP, Shapley Additive Explanations; RF, Random Forest; ET, Extra Trees (classifier); XGB, Extreme Gradient Boosting

any dispensings of either drug decreased the likelihood. In other words: having rofecoxib and celecoxib dispensings on average increased the likelihood of an adverse outcome prediction, and having no such dispensings of these drugs on average decreased or had little effect on the likelihood (in both LIME and SHAP).

4 DISCUSSION

Our study showed that tree-based ML models trained on linked administrative datasets, in tandem with XAI techniques, have the potential to act as an ‘early warning system’ for per-patient ACS related adverse outcomes and for harmful drugs. To the best of our knowledge, this is the first study to demonstrate this using XAI.

The results of our feature importance analysis show that sex and age are ranked highly by MDI, MDA, and SHAP — which is expected, as these are the most important confounding variables in clinical and epidemiological studies. Certain C class drugs (e.g. digoxin, glyceryl trinitrate, isosorbide mononitrate, and furosemide) and comorbidities (see Figure 3 and Appendix A) are consistently reported as being highly important across all feature importance measures, which suggests some level of model independent feature importance. Importantly, the M class drugs celecoxib, rofecoxib, and alendronic acid repeatedly appear as important features across MDI, MDA, and SHAP analyses.

The LIME feature importance scores are inconsistent with the other measures for certain features (see Figure 3). A potential explanation is the variance across multiple consecutive runs in LIME [32] — features which were ranked highly in one run could be ranked lower in another [8]. Despite this, LIME has been shown to be at least as stable as SHAP for highly ranked features [9]. Our results agree



Fig. 3. Names of the features used to predict an ACS related adverse outcome, with feature importance scores (MDI, MDA, LIME, and SHAP) averaged across the RF, ET, and XGB models (to reduce cross-model variance). Sex and age are rendered in dark blue, C class drug history features in light blue, M class drug history features in magenta (with celecoxib and rofecoxib highlighted in red), comorbidities in green, and random forest features in black. In all importance measures other than LIME, the key confounders sex and age are identified as important features, and certain C class drugs, M class drugs, and ICD-10-AM codes are consistently identified as important in predicting an ACS related to the adverse outcome. Note the high importance of celecoxib (M01AH01) and rofecoxib (M01AH02) dispensings when compared to other M class drugs under MDI, MDA, and SHAP analysis (this is shown numerically in Table 3). All features are described in Appendix A. Image best viewed in colour. MDA, Mean Decrease in Impurity; MDA, Mean Decrease in Accuracy; LIME, Local Model Agnostic Explanations; SHAP, Shapley Additive Explanations; RF, Random Forest; ET, Extra Trees (classifier); XGB, Extreme Gradient Boosting; ACS, acute coronary syndrome; ICD, International Classification of Disease.

The Effect of Being Dispensed M01AH01 (celecoxib) and M01AH02 (rofecoxib) on the Likelihood of a Predicted ACS Related Adverse Outcome

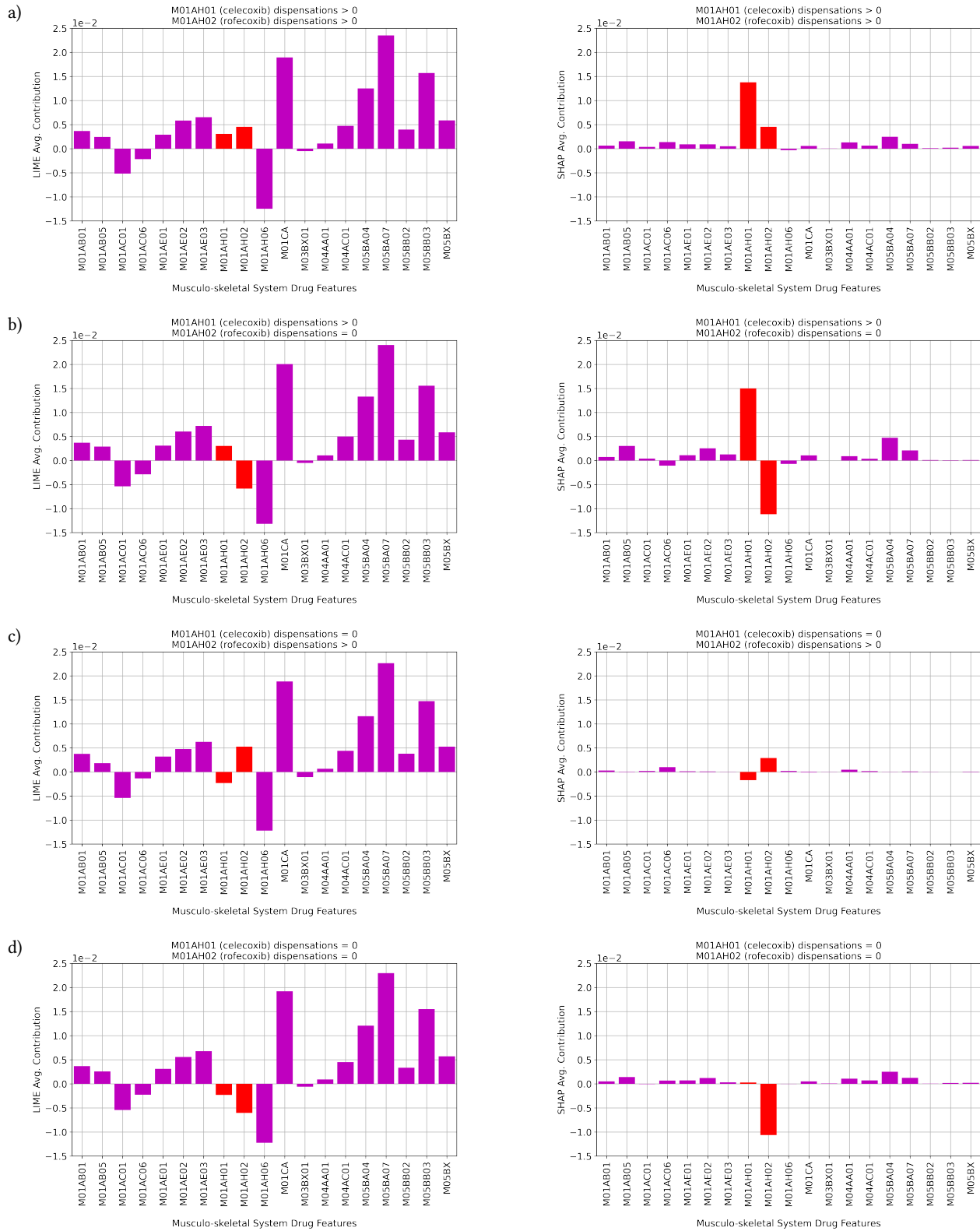


Fig. 4. Dividing the test datasets into strata where an individual was a) dispensed celecoxib and rofecoxib, b) dispensed celecoxib and not rofecoxib, c) not dispensed celecoxib and dispensed rofecoxib, and d) where neither drug was dispensed. The contribution of M class drug history features under LIME analysis (left column) and SHAP analysis (right column) are presented. If individuals have been dispensed celecoxib or rofecoxib this on average resulted in an increased likelihood of a predicted ACS related adverse outcome. If an individual had not been dispensed rofecoxib or celecoxib, then this on average resulted in a near zero or decreased likelihood of a predicted ACS related adverse outcome. Note that, on average, the other M class drug dispensing events did not vary across these subsets, so we do not expect their feature scores to vary across rows a), b), c), and d). Celecoxib (M01AH01) and rofecoxib (M01AH02) are shown in red. M class drug codes are presented in Table 7.

with this: the highly ranked comorbidity features are consistently ranked highly across all feature importance measures.

Random features were included because by definition they cannot have any predictive power — nevertheless, the MDI analysis ranked these features as important. MDI measures have a bias whereby variables with a large number of categories or potential values (high cardinality) are ranked as more important [30]. It is thereby expected that an impurity based approach will inflate the importance of random features. Moreover, MDI feature importance scores are calculated over the decision trees generated by the training dataset, so the importance of non-predictive features may be inflated. Under MDA, these high feature importance scores are reduced as the permutation importance scores are computed over a held out test set (Figure 3).

Each of our feature importance analyses demonstrate that celecoxib and rofecoxib are important when predicting ACS based adverse outcomes, or more specifically, that they actually provide a positive probability contribution to ACS based adverse outcome predictions (see Figure 3). For MDI and MDA, celecoxib and rofecoxib are ranked as the most important M class drugs when making ACS based adverse outcomes predictions. LIME and SHAP analysis shows that both drugs contribute to ACS related adverse outcomes predictions, and SHAP analysis further ranks them as the second and third *most* contributing M class drugs. However, LIME analysis heavily mutes the importance of these features compared to SHAP, greatly reducing the magnitude of their on-average contributions.

Our stratified analysis (see Figure 4 and Table 3) show more detailed results: having *any* celecoxib dispensings in an individual’s drug history increases the likelihood of an ACS related adverse outcome prediction (M01AH01 / celecoxib’s contribution is positive in Figure 4 rows a and b), and *not having any* celecoxib dispensings decreases or does not impact the likelihood of an ACS related adverse outcome prediction (M01AH01 / celecoxib’s contribution is negative or near-zero in Figure 4 rows c and d). In other words, the presence of celecoxib dispensing events increases the likelihood of a positive ACS prediction independent of rofecoxib dispensing events.

This is the equivalent of the counterfactual in the epidemiological theory of causality. The counterfactual conditionals are of the form “if A had not occurred, then C would not have occurred”. This is exactly what is observed in Figure 4. These results provide more robust epidemiological evidence of the associations of celecoxib and rofecoxib with the outcomes.

We acknowledge the utility of existing statistical methods in pharmacovigilance. For example, Sequence Symmetry Analysis (SSA) has been determined to be a promising solution when compared to other quantitative methods such as Reporting Odds Ratio (ROR), Proportional Reporting Ratio (PRR), and Bayesian techniques [15, 16]. SSA considers the distribution of diseases and drugs, before and after initiation of treatment for an adverse event. Asymmetry in these distributions indicate that adverse events may be due to drug supply [13]. SSA’s time to signal detection for rofecoxib-induced myocardial infarction was within 1-3 years of market entry, whereas it took 5-7 years after market entry for trial results to lead to warnings and withdrawals of the drugs [16]. Despite this, there are limitations: in these investigations there are no adverse event signals which can be linked from a joint database; the signals are deduced from

dispensing data only — e.g. furosemide initiation being used as an indicator of heart failure [18]. Using joint databases is more reliable as administrative data entries can validate if a comorbidity did actually occur. Moreover, XAI is better suited for domains which are already using ML-based approaches.

The administrative data used in this study has limitations. By definition, administrative data only includes information which is pertinent to administration. Clinical features which may impact the likelihood of a patient having an ACS related adverse outcome may not be present, and rich clinical information is reduced to ICD-10-AM codes. Also, there were assumptions which we had to apply — for example, we assumed that patients who are dispensed a given drug actually consume it. These shortcomings may have impacted the predictive performance of our models (Table 1). Moreover, the RF, ET, and XGB in this study converged to similar performances, suggesting that there may be a limit to the predictive performance which can be attained using these datasets. Indeed, other ML based predictors trained on administrative data have reached similar performance limits [2, 33].

Further potential research to progress the application of ML techniques in pharmacovigilance include the testing of more diverse ML models (and studies into their inductive biases), benchmarking these methods against other datasets that include more clinical data, investigating additional XAI algorithms [4], using the feature importance scores to iteratively reduce the full set of features, and handling multicollinear features whilst maintaining interpretability. Counterfactual examples may represent an interesting XAI approach to providing transparency in the pharmacovigilance domain, but calculating such explanations may be intractable for high-dimensionality datasets [34].

The strength of our study was the use of multiple linked administrative datasets that cover the whole-of-population. Another strength was the *validation* of feature importances scoring methods against features that have somewhat ‘known’ importances (e.g., it is known that rofecoxib increases the risk of ACS, and that random features are unimportant). Ultimately, we believe that this work highlights the utility of XAI in further analysing trained AI models in challenging domains, and in cases where performance may be constrained due to dataset limitations.

4.1 Conclusion

Tree-based ML models trained on linked administrative datasets, in tandem with XAI techniques, have the potential to act as an ‘early warning system’ for per-patient ACS related adverse outcomes and for harmful drugs in a pharmacovigilance monitoring system. MDA and SHAP methods exceed MDI and LIME methods in identifying known harmful drugs, key confounding variables, and random features. With the appropriate infrastructure and additional clinical data, these algorithms could provide an autonomous method of monitoring adverse outcomes from medications at the population level. This represents a valuable addition to the existing statistical techniques which are currently used and would be the next step in progressing towards a real-time pharmacovigilance monitoring system.

4.2 Author contributions

FM.S., G.D. conceived the study and provided clinical interpretation. IR.W. prepared the data based on a data preparation approach originally implemented by J.L.. IR.W. conducted the experiments. M.B. contributed to the design of machine learning and the use of explainable artificial intelligence. J.L. and L.W. contributed to fortnightly discussions which were led by FM.S., which shaped this work. IR.W, FM.S, J.L, and L.W have access to the underlying data and have verified it. FM.S. contributed to the conception, study design, data acquisition, funding, analysis, and supervision of IR.W.. All co-authors critically revised the work and gave final approval and agreed to be accountable for all aspects of the work ensuring integrity and accuracy.

4.3 Ethics statement

This study complies with the Declaration of Helsinki. Human Research Ethics Committee approvals were received from the Western Australian Department of Health (#2011/62); the Australian Department of Health (XJ-16); and the University of Western Australia (RA/4/1/1130).

4.4 Data sharing statement

We will consider requests for data sharing on an individual basis, with the aim to share data whenever possible for appropriate research purposes. However, this research project uses data obtained from a third-party source under strict privacy and confidentiality agreements from the Western Australian Department of Health (State) and Australian Department of Health (Federal) databases, which are governed by their ethics committees and data custodians. The data were provided after approval was granted from their standard application processes for access to the linked datasets. Therefore, any requests to share these data with other researchers will be subject to formal approval from the third-party ethics committees and data custodian(s). Researchers interested in these data should contact the Data Services Team at the Data Linkage Branch of the Western Australian Department of Health (www.datalinkage-wa.org.au/contact-us).

4.5 Competing interests

Girish Dwivedi reports personal fees from Pfizer, Amgen, Astra Zeneca and Artrya Pty Ltd, all of which are outside the submitted work. No other competing interests were declared.

ACKNOWLEDGMENTS

We thank the following institutions and groups for providing the data used in this study: staff at the WA Data Linkage Branch and data custodians of the WA Department of Health Inpatient Data Collections and Registrar General for access to and provision of the State linked data; the Australian Department of Health for the cross-jurisdictional linked PBS data; the Victorian Department of Justice and Regulation for the cause of death data held in the National Coronial Information System. We also thank the University of WA for funding this work through the 2019 FHMS research grant.

REFERENCES

- [1] Schmider, J. *et al.* Innovation in Pharmacovigilance: Use of Artificial Intelligence in Adverse Event Case Processing. *Clinical Pharmacology & Therapeutics* **105**, 954–961 (2019). URL <https://onlinelibrary.wiley.com/doi/abs/10.1002/cpt.1255>.
- [2] Han, S. S., Azad, T. D., Suarez, P. A. & Ratliff, J. K. A machine learning approach for predictive models of adverse events following spine surgery. *The Spine Journal* **19**, 1772 – 1781 (2019). URL <http://www.sciencedirect.com/science/article/pii/S1529943019308356>.
- [3] Das, A. & Rad, P. Opportunities and challenges in explainable artificial intelligence (xai): A survey. *ArXiv abs/2006.11371* (2020).
- [4] Ribeiro, M. T., Singh, S. & Guestrin, C. Anchors: High-precision model-agnostic explanations. In *AAAI Conference on Artificial Intelligence (AAAI)* (2018).
- [5] Ribeiro, M. T., Singh, S. & Guestrin, C. "why should I trust you?": Explaining the predictions of any classifier. *CoRR abs/1602.04938* (2016). URL <http://arxiv.org/abs/1602.04938>.
- [6] Lundberg, S. & Lee, S. A unified approach to interpreting model predictions. *CoRR abs/1705.07874* (2017). URL <http://arxiv.org/abs/1705.07874>.
- [7] Lai, V., Cai, J. Z. & Tan, C. Many faces of feature importance: Comparing built-in and post-hoc feature importance in text classification. *CoRR abs/1910.08534* (2019). URL <http://arxiv.org/abs/1910.08534>.
- [8] Man, X. & Chan, E. P. The best way to select features? comparing mda, lime, and shap. *The Journal of Financial Data Science* (2020).
- [9] Dieber, J. & Kirrane, S. Why model why? assessing the strengths and limitations of lime (2020). 2012.00093.
- [10] Singh, D. Merck withdraws arthritis drug worldwide. *BMJ (Clinical research ed.)* **329**, 816 (2004).
- [11] Painful lessons. *Nature Structural & Molecular Biology* **12**, 205–205 (2005). URL <https://doi.org/10.1038/nsmb0305-205>.
- [12] Lai, E. C.-C. *et al.* Sequence symmetry analysis in pharmacovigilance and pharmacoepidemiologic studies. *European Journal of Epidemiology* **32** (2017).
- [13] Tsiropoulos, I., Andersen, M. & Hallas, J. Adverse events with use of antiepileptic drugs: A prescription and event symmetry analysis. *Pharmacoepidemiology and drug safety* **18**, 483–91 (2009).
- [14] Hallas, J. Evidence of depression provoked by cardiovascular medication: A prescription sequence symmetry analysis. *Epidemiology* **7**, 478–484 (1996). URL <https://doi.org/10.1097%2F00001648-199609000-00005>.
- [15] Curtis, J. *et al.* Adaptation of bayesian data mining algorithms to longitudinal claims data. *Medical care* **46**, 969–75 (2008).
- [16] Wahab, I., Pratt, N., Kalisch Ellett, L. & Roughead, E. Comparing time to adverse drug reaction signals in a spontaneous reporting database and a claims database: A case study of rofecoxib-induced myocardial infarction and rosiglitazone-induced heart failure signals in australia. *Drug safety: an international journal of medical toxicology and drug experience* **37** (2013).
- [17] Wahab, I., Pratt, N., Wiese, M., Kalisch Ellett, L. & Roughead, E. The validity of sequence symmetry analysis (ssa) for adverse drug reaction signal detection. *Pharmacoepidemiology and drug safety* **22** (2013).
- [18] Wahab, I. A., Pratt, N. L., Ellett, L. K. & Roughead, E. E. Sequence symmetry analysis as a signal detection tool for potential heart failure adverse events in an administrative claims database. *Drug safety* **39**, 347–354 (2016). URL <https://doi.org/10.1007/s40264-015-0391-8>.
- [19] Holman, D., Bass, A., Rouse, I. & Hobbs, M. Population-based linkage of health records in western australia: development of a health services research linked database. *Australian & New Zealand Journal of Public Health* **23**, 453–459 (1999).
- [20] Paige, E., Kemp-Casey, A., Korda, R. & Banks, E. Using australian pharmaceutical benefits scheme data for pharmacoepidemiological research: Challenges and approaches. *Public Health Research and Practice* **25** (2015).
- [21] Lemaitre, G., Nogueira, F. & Aridas, C. K. Imbalanced-learn: A python toolbox to tackle the curse of imbalanced datasets in machine learning. *The Journal of Machine Learning Research* **18**, 559–563 (2017).
- [22] Hasanin, T. & Khoshgoftaar, T. The effects of random undersampling with simulated class imbalance for big data. In *2018 IEEE International Conference on Information Reuse and Integration (IRI)*, 70–79 (IEEE, 2018).
- [23] Breiman, L. Random Forests. *Machine Learning* **45**, 5–32 (2001). URL <https://doi.org/10.1023/A:1010933404324>.
- [24] Geurts, P., Ernst, D. & Wehenkel, L. Extremely randomized trees. *Mach. Learn.* **63**, 3–42 (2006). URL <https://doi.org/10.1007/s10994-006-6226-1>.
- [25] Chen, T. & Guestrin, C. Xgboost: A scalable tree boosting system. *CoRR abs/1603.02754* (2016). URL <http://arxiv.org/abs/1603.02754>.
- [26] Shwartz-Ziv, R. & Armon, A. Tabular data: Deep learning is not all you need. *arXiv preprint arXiv:2106.03253* (2021).
- [27] Snoek, J., Larochelle, H. & Adams, R. P. Practical bayesian optimization of machine learning algorithms. In Pereira, F., Burges, C. J. C., Bottou, L. & Weinberger, K. Q. (eds.) *Advances in Neural Information Processing Systems*, vol. 25, 2951–2959 (Curran Associates, Inc., 2012). URL <https://proceedings.neurips.cc/paper/2012/file/05311655a15b75fab86956663e1819cd-Paper.pdf>.

- [28] Roth, H. R. *et al.* Deeporgan: Multi-level deep convolutional networks for automated pancreas segmentation. In Navab, N., Hornegger, J., Wells, W. M. & Frangi, A. (eds.) *Medical Image Computing and Computer-Assisted Intervention – MICCAI 2015*, 556–564 (Springer International Publishing, Cham, 2015).
- [29] Louppe, G. Understanding random forests: From theory to practice (2015). 1407.7502.
- [30] Altmann, A., Tološi, L., Sander, O. & Lengauer, T. Permutation importance: a corrected feature importance measure. *Bioinformatics* **26**, 1340–1347 (2010).
- [31] Laugel, T., Renard, X., Lesot, M., Marsala, C. & Detyniecki, M. Defining locality for surrogates in post-hoc interpretability. *CoRR abs/1806.07498* (2018). URL <http://arxiv.org/abs/1806.07498>. 1806.07498.
- [32] Alvarez-Melis, D. & Jaakkola, T. S. On the robustness of interpretability methods. *CoRR abs/1806.08049* (2018). URL <http://arxiv.org/abs/1806.08049>. 1806.08049.
- [33] Brignone, E., Fargo, J. D., Blais, R. K. & v Gundlapalli, A. Applying machine learning to linked administrative and clinical data to enhance the detection of homelessness among vulnerable veterans. In *AMIA Annual Symposium Proceedings*, vol. 2018, 305 (American Medical Informatics Association, 2018).
- [34] Ramon, Y., Martens, D., Provost, F. & Evgeniou, T. A comparison of instance-level counterfactual explanation algorithms for behavioral and textual data: Sedic, lime-c and shap-c. *Advances in Data Analysis and Classification* 1–19 (2020).

A FEATURE LOOKUP TABLES AND CODE DESCRIPTIONS

Table 4. Descriptions of the features ‘sex’, ‘age’, ‘rand float’, and ‘rand int’.

Feature	Description
sex	The individual’s sex. The values ‘1’, and ‘2’ represent male and female. It was not possible to consider other values in this study, due to their low sample size.
age	The individual’s age in years.
rand float	A random floating point number in the range 0 – 1.
rand int	A random integer in the range 0 – 157 inclusive (the number of features considered in the study).

Table 5. Drug names of the ATC codes for the C class drugs C01AA05 – C09AA10. In this study, the features corresponding to these codes represent the number of dispensings that an individual had for these drugs in the drug history period.

ATC code	Drug name
C01AA05	digoxin
C01BC04	flecainide
C01BD	Antiarrhythmics, class III
C01BD01	amiodarone
C01DA02	glyceryl trinitrate
C01DA14	isosorbide mononitrate
C01DX16	nicorandil
C02AB01	<i>l</i> -methyldopa
C02AC01	clonidine
C02CA01	prazosin
C03AA01	bendroflumethiazide
C03AA03	hydrochlorothiazide
C03BA11	indapamide
C03CA01	furosemide
C03DA01	spironolactone
C03DB01	amiloride
C03EA01	hydrochlorothiazide & potassium-sparing agents
C07AA03	pindolol
C07AA05	propranolol
C07AB02	metoprolol
C07AB03	atenolol
C07AB07	bisoprolol
C07AG02	carvedilol
C08CA01	amlodipine
C08CA02	felodipine
C08CA05	nifedipine
C08CA13	lercanidipine
C08DA01	verapamil
C08DB01	diltiazem
C09AA01	captopril
C09AA02	enalapril
C09AA03	lisinopril
C09AA04	perindopril
C09AA05	ramipril
C09AA06	quinapril
C09AA09	fosinopril
C09AA10	trandolapril

Table 6. Drug names of the ATC codes for the C class drugs C09BA02 – C10BX03. In this study, the features corresponding to these codes represent the number of dispensings that an individual had for these drugs in the drug history period.

ATC code	Drug name
C09BA02	enalapril and diuretics
C09BA04	perindopril and diuretics
C09BA06	quinapril and diuretics
C09BA09	fosinopril and diuretics
C09CA02	eprosartan
C09CA04	irbesartan
C09CA06	candesartan
C09CA07	telmisartan
C09DA02	eprosartan and diuretics
C09DA04	irbesartan and diuretics
C09DA06	candesartan and diuretics
C09DA07	telmisartan and diuretics
C10AA01	simvastatin
C10AA03	pravastatin
C10AA04	fluvastatin
C10AA05	atorvastatin
C10AA07	rosuvastatin
C10AB04	gemfibrozil
C10AB05	fenofibrate
C10AX09	ezetimibe
C10BA02	simvastatin and ezetimibe
C10BX03	atorvastatin and amlodipine

Table 7. Drug names of the ATC codes for all the M class drugs considered in this study. In this study, the features corresponding to these codes represent the number of dispensings that an individual had for these drugs in the drug history period.

ATC code	Drug name
M01AB01	indometacin
M01AB05	diclofenac
M01AC01	piroxicam
M01AC06	meloxicam
M01AE01	ibuprofen
M01AE02	naproxen
M01AE03	ketoprofen
M01AH01	celecoxib
M01AH02	rofecoxib
M01AH06	lumiracoxib
M01CA	Quinolines, antirheumatic drugs
M03BX01	baclofen
M04AA01	allopurinol
M04AC01	colchicine
M05BA04	alendronic acid
M05BA07	risedronic acid
M05BB02	risedronic acid and calcium, sequential
M05BB03	alendronic acid and colecalciferol
M05BX	Other drugs affecting bone structure and mineralization in ATC

Table 8. Descriptions of the ICD-10-AM codes I20.0 – I50.9. In this study, the features corresponding to these codes represent the number of hospitalisations that an individual had due to these conditions in the comorbidity history period.

ICD-10	Description
I20.0	Unstable angina
I20.1	Angina pectoris with documented spasm
I20.8	Other forms of angina pectoris
I20.9	Angina pectoris, unspecified
I21.0	ST elevation myocardial infarction of anterior wall
I21.1	ST elevation myocardial infarction of inferior wall
I21.2	ST elevation myocardial infarction of other sites
I21.3	ST elevation myocardial infarction of unspecified site
I21.4	Non-ST elevation myocardial infarction
I21.9	Acute myocardial infarction, unspecified
I22.0	Subsequent ST elevation and non-ST elevation myocardial infarction
I22.1	Subsequent ST elevation myocardial infarction of inferior wall
I22.8	Subsequent ST elevation myocardial infarction of other sites
I22.9	Subsequent ST elevation myocardial infarction of unspecified site
I23.0	Certain current complications following ST elevation and non-ST elevation myocardial infarction (within the 28 day period)
I23.1	Atrial septal defect as current complication following acute myocardial infarction
I23.2	Ventricular septal defect as current complication following acute myocardial infarction
I23.3	Rupture of cardiac wall without hemopericardium as current complication following acute myocardial infarction
I23.5	Rupture of papillary muscle as current complication following acute myocardial infarction
I23.6	Thrombosis of atrium, auricular appendage, and ventricle as current complications following acute myocardial infarction
I23.8	Other current complications following acute myocardial infarction
I24.0	Other acute ischemic heart diseases
I24.1	Dressler’s syndrome
I24.8	Other forms of acute ischemic heart disease
I24.9	Acute ischemic heart disease, unspecified
I25.0	Chronic ischemic heart disease
I25.1	Atherosclerotic heart disease of native coronary artery
I25.2	Old myocardial infarction
I25.3	Aneurysm of heart
I25.4	Coronary artery aneurysm and dissection
I25.5	Ischemic cardiomyopathy
I25.6	Silent myocardial ischemia
I25.8	Other forms of chronic ischemic heart disease
I25.9	Chronic ischemic heart disease, unspecified
I50.0	Heart failure
I50.1	Left ventricular failure, unspecified
I50.9	Heart failure, unspecified

Table 9. Descriptions of the ICD-10-AM codes I60.0 – I64, K92.0 – K92.2, and R58. In this study, the features corresponding to these codes represent the number of hospitalisations that an individual had due to these conditions in the comorbidity history period.

ICD-10	Description
I60.0	Nontraumatic subarachnoid hemorrhage from unspecified carotid siphon and bifurcation
I60.1	Nontraumatic subarachnoid hemorrhage from unspecified middle cerebral artery
I60.2	Nontraumatic subarachnoid hemorrhage from anterior communicating artery
I60.3	Nontraumatic subarachnoid hemorrhage from unspecified posterior communicating artery
I60.4	Nontraumatic subarachnoid hemorrhage from basilar artery
I60.5	Nontraumatic subarachnoid hemorrhage from unspecified vertebral artery
I60.6	Nontraumatic subarachnoid hemorrhage from other intracranial arteries
I60.7	Nontraumatic subarachnoid hemorrhage from unspecified intracranial artery
I60.8	Other nontraumatic subarachnoid hemorrhage
I60.9	Nontraumatic subarachnoid hemorrhage, unspecified
I61.0	Nontraumatic intracerebral hemorrhage in hemisphere, subcortical
I61.1	Nontraumatic intracerebral hemorrhage in hemisphere, cortical
I61.2	Nontraumatic intracerebral hemorrhage in hemisphere, unspecified
I61.3	Nontraumatic intracerebral hemorrhage in brain stem
I61.4	Nontraumatic intracerebral hemorrhage in cerebellum
I61.5	Nontraumatic intracerebral hemorrhage, intraventricular
I61.6	Nontraumatic intracerebral hemorrhage, multiple localized
I61.8	Other nontraumatic intracerebral hemorrhage
I61.9	Nontraumatic intracerebral hemorrhage, unspecified
I62.0	Nontraumatic subdural hemorrhage, unspecified
I62.1	Nontraumatic extradural hemorrhage
I62.9	Nontraumatic intracranial hemorrhage, unspecified
I63.0	Cerebral infarction due to thrombosis of unspecified precerebral artery
I63.1	Cerebral infarction due to embolism of unspecified precerebral artery
I63.2	Cerebral infarction due to unspecified occlusion or stenosis of unspecified precerebral arteries
I63.3	Cerebral infarction due to thrombosis of unspecified cerebral artery
I63.4	Cerebral infarction due to embolism of unspecified cerebral artery
I63.5	Cerebral infarction due to unspecified occlusion or stenosis of unspecified cerebral artery
I63.6	Cerebral infarction due to cerebral venous thrombosis, nonpyogenic
I63.8	Other cerebral infarction
I63.9	Cerebral infarction, unspecified
I64	Stroke, not specified as haemorrhage or infarction
K92.0	Hematemesis
K92.1	Melena
K92.2	Gastrointestinal hemorrhage, unspecified
R58	Hemorrhage, not elsewhere classified

B HYPERPARAMETER SEARCHES

Table 10. The range of values that the hyperparameters could take during our RF and ET hyperparameter optimisation.

Hyperparameter	Search distribution
n_estimators	8 – 32
max_features	‘auto’, ‘sqrt’
max_depths	8 – 64, no limit
min_samples_split	2 – 12
min_samples_leaf	2 – 8
bootstrap	True, False

Table 11. The range of values that the hyperparameters could take during our XGB hyperparameter optimisation.

Hyperparameter	Search distribution
booster	‘gbtree’, ‘gblinear’
max_depth	2 – 32, no limit
sampling_method	‘uniform’, ‘gradient_based’
alpha	0, 0.1, 0.5
lambda	0.8, 1, 1.2
grow_policy	‘depthwise’, ‘lossguide’